Electronic Supplementary Information

Experimental

Chemical reagents

Methanol (99%), zinc nitrate hexahydrate (ACS reagent, ≥98%) were purchased from Sigma Aldrich. 2-methylimidazole (2-MIM) was obtained from Sinopharm Chemical Reagent Co., Ltd. Cupric nitrate and lead nitrate were purchased from Aladdin Chemical Co., Ltd. All chemicals were used as received without any further purification. Deionized water was used in all experiments.

Fabrication of ZIF-8-x

The general ZIF-8-0 was synthesized through an improved reported method [1]. First, 0.4 g $Zn(NO_3)_2$•$6H_2O$ was mixed with 9.6 mL water; after the solid was totally dissolved in the solvent, 0.5 g 2-MIM with 16 mL water was added into the solution. The mixture was stirred continuously for 30 min. The product was collected by centrifuging the mixture at 6000 rpm for 10 min. Afterwards, the product was washed several times with water and then dried in a vacuum oven. The different dosages of $Zn(NO_3)_2$ and 2-MIM for various adsorbents (ZIF-8-z, z presents the mass ratio of zinc nitrate and 2-MIM) were summarized in **Table S1**. ZIF-8-x with different morphology were synthesized by using different contents of water (varying from 0% to 100%) in the aforementioned procedure. Schematic diagram of the experimental setup is depicted in **Fig. S1**.

Characterization

Field emission scanning electron microscope (SEM) image was taken by an S-

4800 (Hitachi, Japan). Powder X-ray diffraction (XRD) patterns was gotten by a powder diffractometer, Bruker D8 Advanced Diffractometer System, which was equipped with Cu Kα radiation (40 kV, 40 mA).The adsorption value was measured with flame atomic absorption spectrometry (FAAS) (Z-2000, Hitachi). X-ray photoelectron spectroscopy (XPS) data were recorded using an Axis Ultra DLD X-ray photoelectron spectrometer equipped with an Al Ka X-ray source (1486.6 eV). The Brunauer-Emmett-Teller (BET) surface area, pore volume and pore size were obtained by a Gemini VII2390 instrument. Thermal gravimetric analysis (TGA) measurements were performed on a NETZSCH STA 449 F3 Thermoanalyzer, and about 15 mg of each sample was used for TGA analysis.

Batch adsorption experiment

To explore the adsorption efficiency of Cu(II) by a series of ZIF-8-x, a batch of adsorption experiment was employed, using cupric nitrate as the source of Cu(II) solutions. Sorption experiments were carried out in Cu(II) aqueous solution (8 mL) incubated with 50 mg/L adsorbents mixed by a rotary shaker.

To explore the influence of pH values on the Cu(II) adsorption of ZIF-8-0, the pH of initial Cu(II) solution (200 mg L^{-1}) was adjusted by 0.1M HCl and 0.1M NaOH solutions in the range of 1.0-5.5. For kinetic studies, typical adsorption experiments were performed under various adsorption time intervals (0-1 h) with the given initial ion concentration in the range of 5-50 mg L^{-1}. The isotherm study was conducted under different temperature from 298 K to 308 K, each isotherm curves were conducted with different initial Cu(II) concentrations ranging from 10 to 300 mg L^{-1}.

The residual Cu(II) concentration in the solution was determined using FAAS.

The adsorption capacity is calculated as follows:

$$q_e = \frac{(C_0 - C_e)V}{m} \qquad (1)$$

In eqn (1), q_e (mg g^{-1}) and C_e (mg L^{-1}) are the adsorption capacity and equilibrium concentration of Cu(II), respectively. V (L) and m (g) in the equation are the volume of Cu(II) solution and the mass of adsorbent, respectively. The removal performance for different ions including Pb(II), Cd(II), Ni(II) and Fe(III) were conducted under the same initial concentration (200 mg L^{-1}), incubated for 1 h to reach adsorption equilibrium.

S1. Schematic diagram

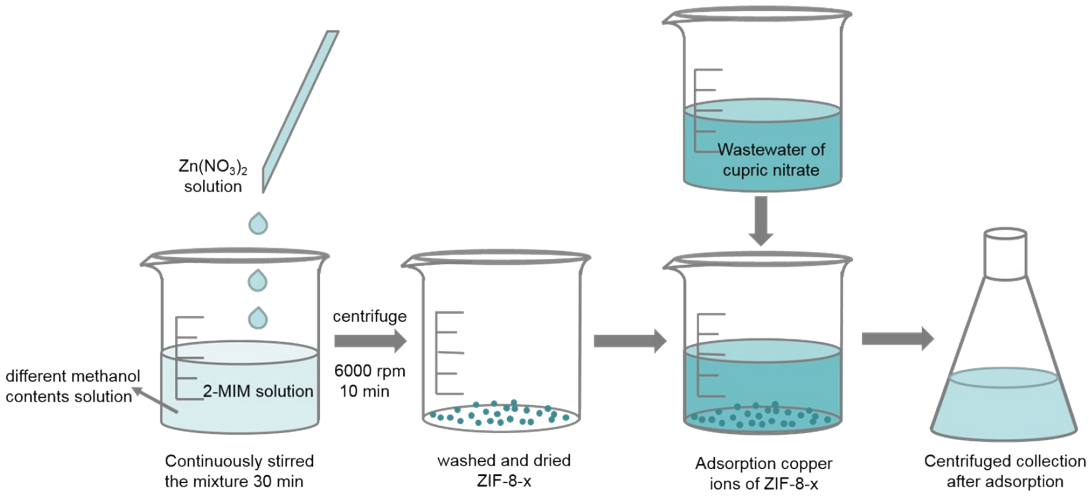

Fig. S1 Schematic diagram of experimental process.

S2. The characteristics and productivity of ZIF-8-z

Table S1. The dosages of $Zn(NO_3)_2$ and 2-MIM for various ZIF-8-z adsorbents

absorbent	$Zn(NO_3)_2$ (g)	2-MIM (g)
ZIF-8-1:5	0.1	0.5
ZIF-8-2:5	0.2	0.5
ZIF-8-3:5	0.3	0.5
ZIF-8-4:5	0.4	0.5
ZIF-8-7:5	0.7	0.5
ZIF-8-10:5	1	0.5
ZIF-8-50:5	5	0.5

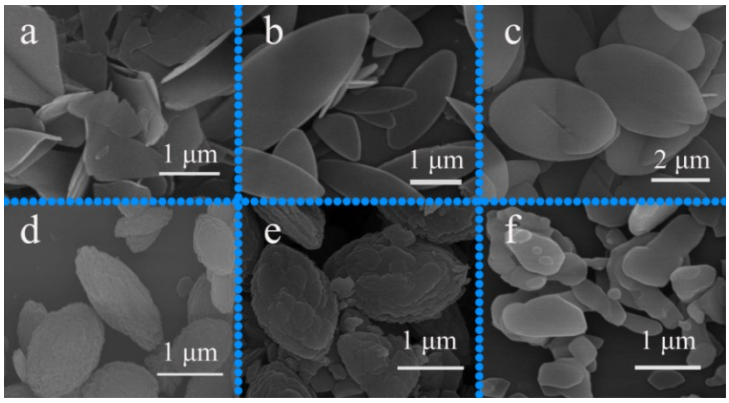

Fig. S2 SEM of various ZIF-8-z, a) ZIF-8-1:5, b) ZIF-8-2:5, c) ZIF-8-4:5, d) ZIF-8-7:5, e) ZIF-8-10:5 and f) ZIF-8-50:5.

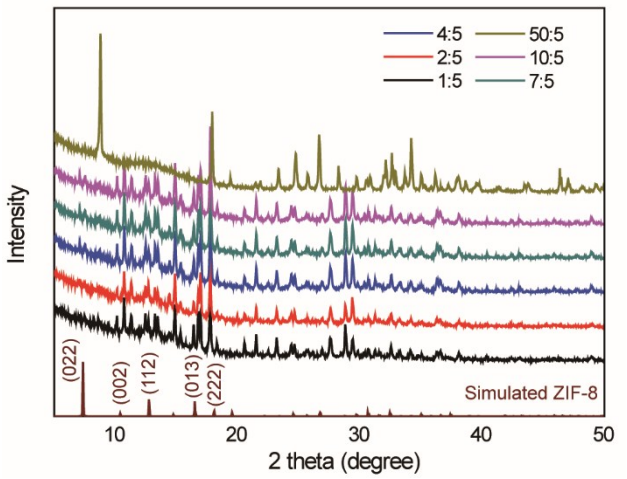

Fig. S3 The XRD patterns of ZIF-8-1:5, ZIF-8-2:5, ZIF-8-4:5, ZIF-8-7:5, ZIF-8-10:5 and ZIF-8-50:5.

Table S2. The productivity for various ZIF-8-z adsorbents.

absorbent	Productivity (%)
ZIF-8-1:5	18.11
ZIF-8-2:5	22.89
ZIF-8-3:5	26.67
ZIF-8-4:5	**29.78**
ZIF-8-7:5	28.64
ZIF-8-10:5	28.18
ZIF-8-50:5	28.21

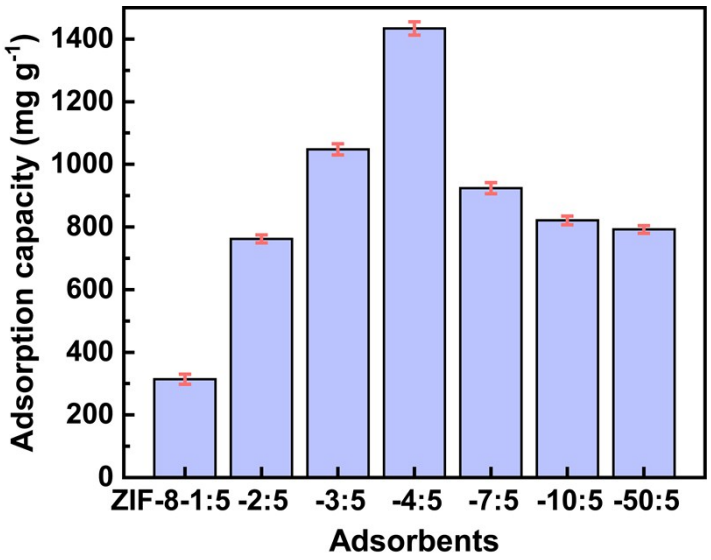

Fig. S4 Adsorption capacities of different ZIF-8-z adsorbents towards Cu(II).

To investigate the effect of Zn(II) concentration on the synthesis of ZIF-8, 6 kinds of ZIF-8-z were prepared in pure water and then characterized. As shown in **Fig. S2**, the concentration of zinc nitrate hexahydrate is a crucial factor to control the morphology and structure of the obtained ZIF-8-z from irregular nanosheet, leaf-shape nanosheet and fusiform nanoparticle to irregular nanoparticle. Correspondingly, as shown in **Fig. S3**, the crystal structure changed from ZIF-8 phase to ZIF-L phase. When the mass ratio of zinc nitrate hexahydrate was lower than 50:5, it shows no significant effect on the crystallinity of the ZIF-8-z. Thereinto, the better productivity ZIF-8-4:5 (29.78%) than other ZIF-8-z were concluded from the productivity results in **Table S2**. Furthermore, because the ZIF-8-4:5 shows better adsorption capacity compared to the other adsorbents in the **Fig. S4**, we choose this mass ratio of zinc nitrate hexahydrate and 2-MIM to further investigate the solvent effect in morphology transformation.

S3. The composition and SEM images of ZIF-8-x

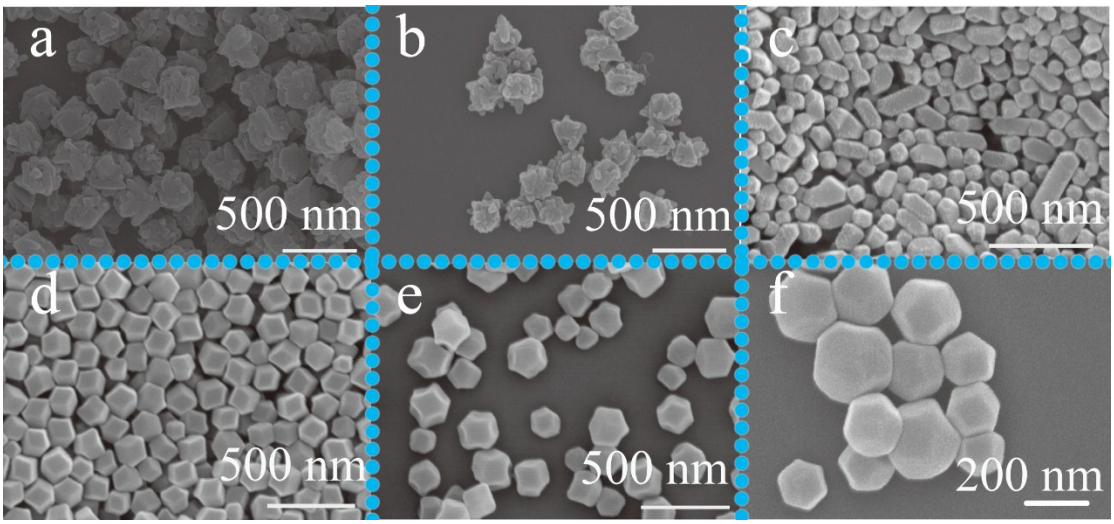

Fig. S5 SEM images of a) ZIF-8-27.5, b) ZIF-8-30, c) ZIF-8-45, d) ZIF-8-55 e) ZIF-8-60 and f) ZIF-8-100.

S4. SEM of ZIF-8-0 prepared under different reaction times

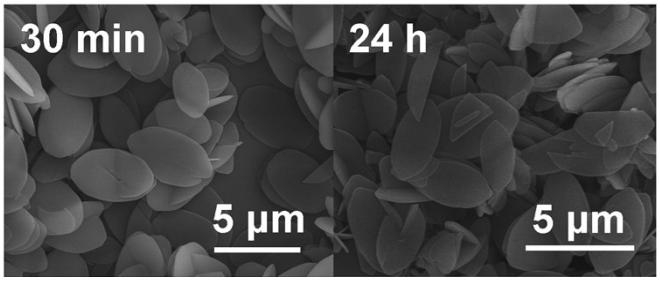

Fig. S6 SEM characterization of ZIF-8-0 prepared under different reaction times.

S5. Viscosity coefficients and dielectric constants of ZIF-8-x solution

Table S3. Viscosity coefficients and dielectric constants of methanol with different content of water.

Solution	Viscosity coefficients (293 K)/ mPas	Dielectric constants (293 K)
0% water	0.59	32.7
10% water	0.66	36.9
20% water	0.88	40.3
30% water	1.02	43.1
40% water	1.11	45.5
50% water	1.17	49.9
60% water	1.15	53.0
70% water	1.07	58.5
80% water	0.98	61.6
90% water	0.92	69.7
Pure Water	1.0	78.5

S6. The Full width at half maxima (FWHM) of ZIF-8-x

Table S4. The Full width at half maxima (FWHM) of ZIF-8-x.

Adsorbents	FWHM (degree)
ZIF-8-0	0.154
ZIF-8-20	0.120
ZIF-8-40	0.230
ZIF-8-50	0.186
ZIF-8-60	0.141
ZIF-8-80	0.105
ZIF-8-100	0.124

S7. Nitrogen sorption isotherms and corresponding parameters of ZIF-8-x

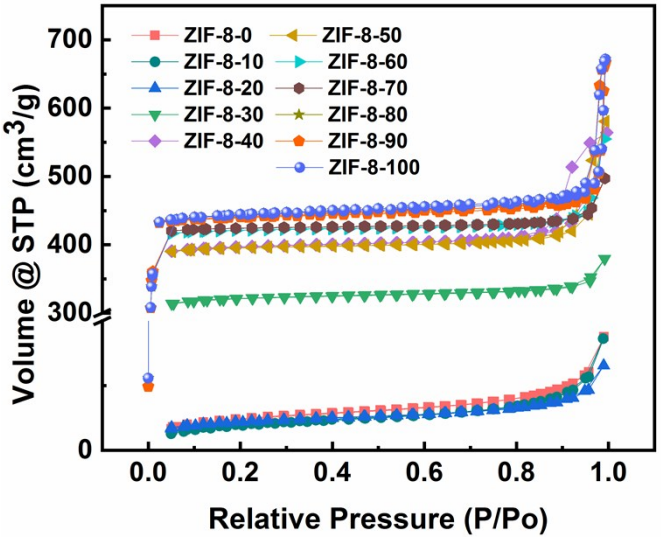

Fig. S7 Nitrogen sorption isotherms of ZIF-8-x nanocrystals.

Table S5. Pore volume of ZIF-8-x nanocrystals.

Adsorbents	Pore volume (cm^3/g)
ZIF-8-0	1.34×10^{-2}
ZIF-8-10	1.26×10^{-2}
ZIF-8-20	1.01×10^{-2}
ZIF-8-30	0.58
ZIF-8-40	0.85
ZIF-8-50	0.87
ZIF-8-60	0.85
ZIF-8-70	0.76
ZIF-8-80	0.72
ZIF-8-90	0.65
ZIF-8-100	0.65

Table S6. BET surface areas of ZIF-8-x nanocrystals.

Adsorbents	BET surface areas (m^2/g)
ZIF-8-0	8.92
ZIF-8-10	8.31
ZIF-8-20	8.00
ZIF-8-30	1.09×10^3
ZIF-8-40	1.35×10^3
ZIF-8-50	1.34×10^3
ZIF-8-60	1.43×10^3
ZIF-8-70	1.44×10^3
ZIF-8-80	1.67×10^3
ZIF-8-90	1.81×10^3
ZIF-8-100	1.82×10^3

S8. Batch adsorption experiments

Table S7. Adsorption capacities of different ZIF-8-x towards Cu(II).

Adsorbents	Adsorption capacity (mg g^{-1})
ZIF-8-0	1439
ZIF-8-20	1364
ZIF-8-40	1308
ZIF-8-50	1174
ZIF-8-60	1152
ZIF-8-80	1121
ZIF-8-100	954

SEM was employed to verify the water stability of the ZIF-8-0, which was conducted by immersing ZIF-8-0 in deionized water for 6 h and then dried it out for further characterization.

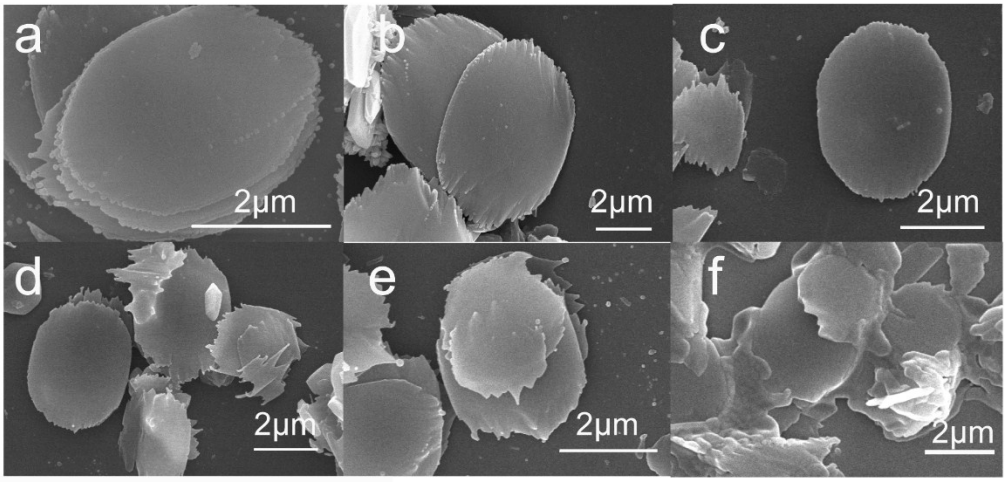

Fig. S8 SEM images of ZIF-8-0 under different pH a) pH=5.5, b) pH=5, c) pH=4, d) pH=3 e) pH=2 and f) pH=1.

Table S8 The pH change on Cu(II) adsorption by ZIF-8-0. Initial Cu(II) concentration: 100 mg/L; adsorbent dosage: 50 mg/L.

Initial pH value	Final pH value
1.15	1.21
2.28	2.37
3.21	3.36
4.13	4.59
5.17	5.61
5.75	6.18

Table S9. Kinetic parameters of Cu(II) adsorption on ZIF-8-0.

copper concentration(mg L^{-1})	pesudo-second-order				pecudo-first-order		
	$q_{e,exp}$	k_2 (g/mg min)	$q_{e,cal}$ (mg g^{-1})	R^2	k_1 (min^{-1})	q_e (mg g^{-1})	R^2
5	97.72	0.065	90.97	0.963	0.87	88.28	0.948
10	212.28	1.486	203.23	0.985	1.01	201.13	0.984
20	462.81	1.75	454.41	0.994	1.10	447.53	0.985
30	627.15	0.0094	619.46	0.991	1.11	613.01	0.984
50	810.44	1.69	801.13	0.994	1.25	787.17	0.985

Table S10. Isotherm parameters of Cu(II)adsorption on ZIF-8-0.

adsorbent	Temperature (K)	Langmuir isotherm			Freundlich isotherm		
		q_m (mg g^{-1})	K_L (L mg^{-1})	R^2	K_f (mg g^{-1})	n	R^2
ZIF-8-0	308	1457.87	0.057	0.971	300.60	3.39	0.969
	303	1336.64	0.034	0.979	194.71	2.89	0.974
	298	1096.28	0.029	0.980	140.29	2.74	0.976

Table S11. Thermodynamic parameters of Cu(II) adsorption on ZIF-8-0.

adsorbent	Temperature (K)	ΔG^0 (J mol^{-1})	ΔH^0 (KJ mol^{-1})	ΔS^0 (J mol^{-1} K^{-1})
ZIF-8-0	298	-3419.94	576.06	15.61
	303	-4145.50		
	308	-4646.69		

Table S12. Cu(II) adsorption capacities and PC values of ZIF-8-0 under different temperatures.

Temperature (K)	Final concentration (mg L^{-1})	Adsorption capacity (mg g^{-1})	Partition coefficient (mg g^{-1} μM^{-1})
298	0.61	187.82	308.41
303	1.479	170.42	115.23
308	2.979	140.42	47.14

As shown in the **Table S12**, the maximum adsorption capacities and Partition coefficient of ZIF-8-0 towards Cu(II) rise obviously with the increase of temperature. We can conclude that the maximal partition coefficient is 308.41 mg g^{-1} μM^{-1}.

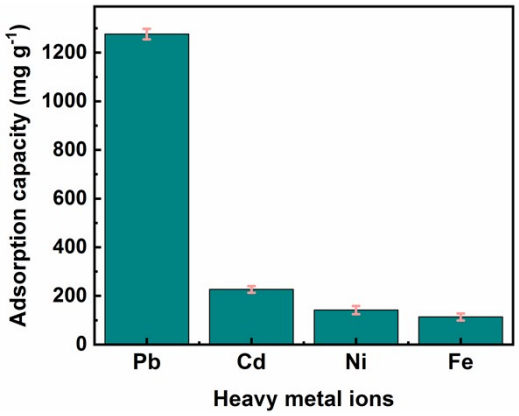

Fig. S9 Adsorption capacity of ZIF-8-0 toward Pb^{2+}, Cd^{2+}, Ni^{2+} and Fe^{3+}.

S9. XPS analysis of ZIF-8-0 before and after adsorption.

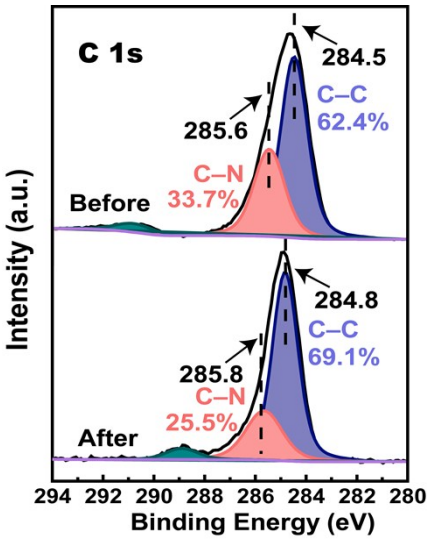

Fig. S10 C 1s peaks of ZIF-8-0 before and after Cu^{2+} adsorption.

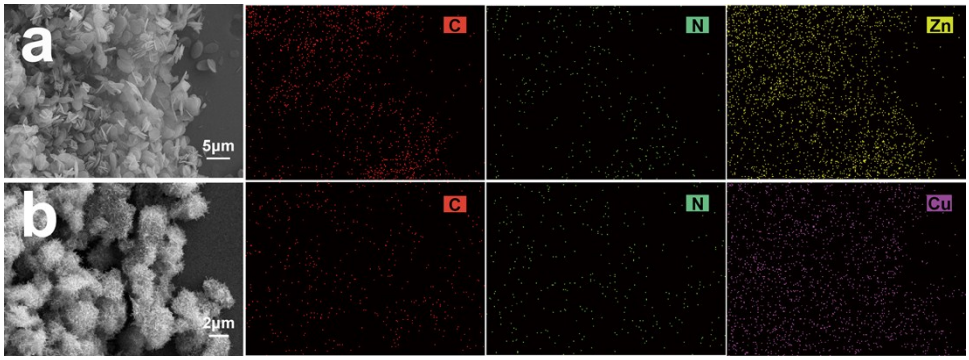

Fig. S11 SEM-EDS mapping of ZIF-8-0 (a) before and (b) after Cu^{2+} adsorption.

Table S13. SEM-EDS analysis of element content before and after adsorption.

Element of ZIF-8-0	Before adsorption	After adsorption
C	36.57%	12.15%
N	22.71%	14.17%
O	5.14%	20.16%
Zn	35.58%	1.83%
Cu	0%	51.69%

Reference

1. R. Chen, J. Yao, Q. Gu, S. Smeets, C. Baerlocher, H. Gu, D. Zhu, W. Morris, O. M. Yaghi and H. Wang, *Chem. Commun.*, 2013, **49**, 9500-9502.